Propagating Radical Termination at High Conversion in Emulsion Polymerization of MMA. Rate Coefficient Determination from ESR Data

S. Fitzwater,* H.-R. Chang,† H.-Y. Parker, and D. G. Westmoreland

Rohm and Haas Company, Spring House, Pennsylvania 19477

Received February 13, 1998; Revised Manuscript Received January 12, 1999

ABSTRACT: Termination rate coefficients for poly(methyl methacrylate) (PMMA) propagating radicals have been determined from ESR measurements of the propagating free radical concentration during batch emulsion polymerization. At conversions ≥∼99%, the termination is clearly second order in radical concentration. At conversions of ∼90−96%, a rapid termination occurs in larger latex particles but not in smaller ones. If we assume that this termination is bimolecular, then the termination rate coefficient is not constant. The rapid termination rate coefficients are up to ∼2 orders of magnitude higher than the very high conversion termination coefficients. Comparison of the termination rate coefficients determined here, those determined by other workers, and predictions from chain-length-dependent termination theory suggest that (1) the high conversion termination is residual or reaction diffusion−chains ends do not move freely but approach each other by adding monomer, (2) the chain-length-dependent termination theory probably overestimates the residual termination coefficient somewhat, and (3) some short−long termination probably occurs early in the rapid termination period. We hypothesize that the rapid termination occurs in the larger particles because of radical distribution inhomogeneity.

Introduction

It is generally accepted that there are two important bimolecular termination mechanisms in free-radical emulsion polymerization. The first of these is short−long termination, in which a radical on a mobile, oligomeric chain reacts with a radical on a long, immobile chain.[1] The second is residual termination, in which radicals on long, immobile chains approach each other by adding monomer until they are close enough to react.[1]

Theory suggests that short−long termination is the dominant termination mechanism throughout most of an emulsion polymerization.[1−3] The reasoning is that although most of the radicals are "longs", short−long termination is so much faster than residual termination that it dominates. This same reasoning explains why short−short termination is often ignored; the short−short and short−long terminations have comparable rate coefficients, but there are many more "longs" than "shorts". So most of the "shorts" terminate "longs", rather than other "shorts".

At very high conversion (and at temperatures below the glass transition temperature, T_g), the short−long termination rate is believed to slow precipitously, tracking the rapid decrease in the diffusion rate of the oligomeric radicals in polymer.[1,4,5] At this point, the rates of short−long and residual termination become comparable. Because there are many more "longs" than "shorts", residual termination dominates at high conversion.

Experimental Data

Data obtained recently can give us further information on termination in PMMA. A previous paper[6] described results of an ESR experiment that measures the concentration of propagating free radicals in batch emulsion polymerization of MMA. The polymerization was initiated using sodium persulfate/sodium sulfoxylate formaldehyde (SSF) at a temperature of 45 °C and allowed to exotherm with a peak temperature of 58−60 °C. The concentration of the propagating free radicals was monitored throughout the polymerization by ESR using a time-sweep experiment in which the magnetic field was set to the frequency of one of the lines of the nine-line spectrum of the PMMA propagating radical. The intensity was measured every 2.6 s, so the experiment gives a very detailed picture of how the propagating radical concentration changes with time.

A typical radical concentration vs time plot for a larger particle size (∼230 nm final diameter) polymerization is shown in Figure 1. The radical concentration, [R•], remains below the detection limit until the T_g of the polymerizing latex rises above the reaction temperature, about 50 min into the polymerization. At this time [R•] increases rapidly, peaks, and then decreases. The decrease is quite rapid at first, but after ∼20−30 min it tails off to a slow, steady decrease which continues for at least 2 h (and probably much longer).

Figure 1 shows data from one of the "long hold" runs described in the earlier paper.[6] In these experiments, the first part of the polymerization and data collection was run with the polymerizing latex flowing through the ESR cell. Then, 60−90 min after the start of the polymerization (well into the decay period and after the rapid termination period for the larger particles), the flow was stopped, and the temperature of the almost completely polymerized latex held in the ESR cell was set to a constant value and the radical concentration monitored for an additional 1−3 h.

In this paper, we will define the following time periods in the radical concentration data as indicated in Figure 1:

ESR signal decay period: from peak [R•] to end of experiment.

Rapid termination period, region 1: from peak [R•] to 20 min after peak [R•], w_p = ∼0.90−0.96.

† Current address: Industrial Technology Research Institute, 321 Kuang Fu Rd., Section 2, Hsinchu, Taiwan 300, ROC.

10.1021/ma980230m CCC: $18.00
Published on Web 04/17/1999

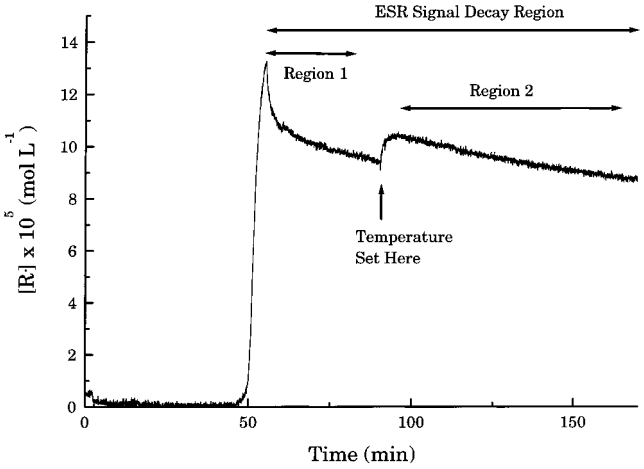

Figure 1. Radical concentration vs time for a polymerization with final particle diameter of 230 nm. The temperature set point indicated is the time at which the temperature of the ESR cell was set to the value for which the termination was to be measured.

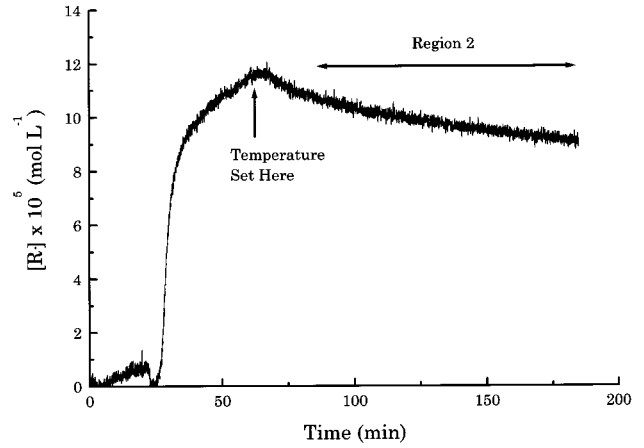

Figure 2. Radical concentration vs time for a polymerization with final particle diameter of 110 nm. The temperature set point indicated is the time at which the temperature of the ESR cell was set to the value for which the termination was to be measured.

Slower termination period, region 2: from ~20 min after the temperature set time (~40−70 min after peak [R•]) to end of experiment, $w_p \geq 0.99$.

As shown in the previous paper,[6] ESR data for smaller particle size polymerizations (final particle diameter ≤120 nm) generally did not show the rapid termination period observed for larger particle size polymerizations. A typical [R•] vs time plot from a "long hold" run for such particles is shown in Figure 2. Note that while there is a decay period, there is a much longer time between the initial [R•] increase and the decay period than in the larger particles. Also, there is only a hint of a rapid termination period, soon after the temperature set time. "Regular" runs for the smaller particles, in which there was no temperature set and [R•] was monitored for ~120 min, did not show any decay period (rapid or slow).[6]

Data from the decay periods for both types of particles can be used to estimate radical termination rate coefficients. The decay period corresponds to high weight fraction of polymer (w_p), typically ≥0.95. So the analysis of data from the decay period gives insight into the termination processes which occur at very high conversion.

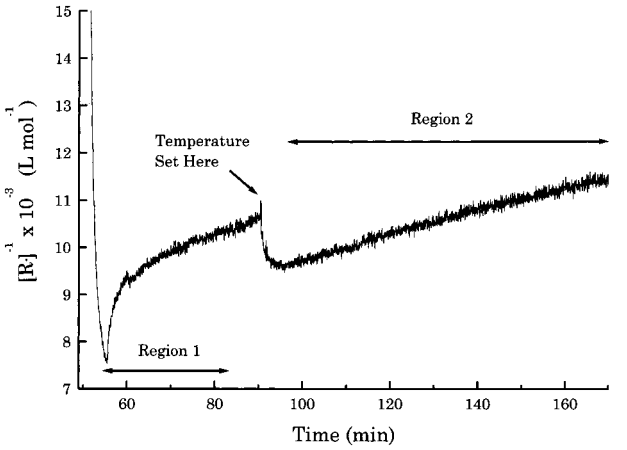

Figure 3. Inverse radical concentration vs time during the decay period, 230 nm PMMA particles.

A cursory analysis of the radical concentration decay data suggests that more than one termination process occurs, at least in the larger particles. Data from region 2 are consistent with residual termination, for both types of particles. Data from region 1 imply a much faster termination, particularly during the period ≤5 min after the radical peak.

Data Analysis and Results: Region 2 (Slower Termination Period)

Figure 3 shows a typical 1/[R•] vs time plot from one of the "long hold" runs for a larger particle size polymerization. There is a linear dependence of 1/[R•] on time throughout region 2. This implies that the termination during this period can be modeled as a bimolecular reaction with constant rate coefficient.

The usual bimolecular termination model with time-independent rate coefficient is

$$d[R^\bullet]/dt = -k_t[R^\bullet]^2 \quad (1)$$

Here, t is time and k_t is the termination rate coefficient. In our experiment, we expect k_t to be essentially time-independent because w_p is nearly constant (varies by ~0.01 or less) throughout the slower termination period. Integration of eq 1 gives

$$1/[R^\bullet] = 1/[R^\bullet]_0 + k_t t \quad (2)$$

We derived values of k_t from the slow termination period data using eq 2 and the SAS nonlinear regression procedure, PROC NLIN.[7]

Long hold experiments were run for 110 and 230 nm particle size polymerizations at 55, 65, and 75 °C. All experiments were run in duplicate and a few in triplicate. The derived k_t values are shown in Table 1. The k_t values for the 110 nm particles are uniformly smaller than the values for the 230 nm particles. The differences between k_t values for the small and large particles are statistically significant. Figure 4 shows an Arrhenius plot for the two different particle sizes. The $\ln(k_t)$ vs inverse temperature dependence looks reasonably linear. Calculated activation energy values are shown in Table 2. The activation energy values for the two particle sizes are statistically indistinguishable.

Data Analysis and Results: Region 1 (Rapid Termination Period)

We have already seen that we cannot model data from region 1 as a bimolecular termination if we assume a

Table 1. Termination Rate Coefficients Derived from Long Hold Runs

particle size (nm)	temp (°C)	run no.	k_t (L mol^{-1} s^{-1})
230	55	1	0.21
		2	0.21
		avg	0.21
	65	1	0.56
		2	0.94
		avg	0.75
	75	1	2.0
		2	1.1
		avg	1.6
110	55	1	0.068
		2	0.17
		3	0.13
		avg	0.12
	65	1	0.30
		2	0.30
		avg	0.30
	75	1	1.3
		2	1.0
		avg	1.2

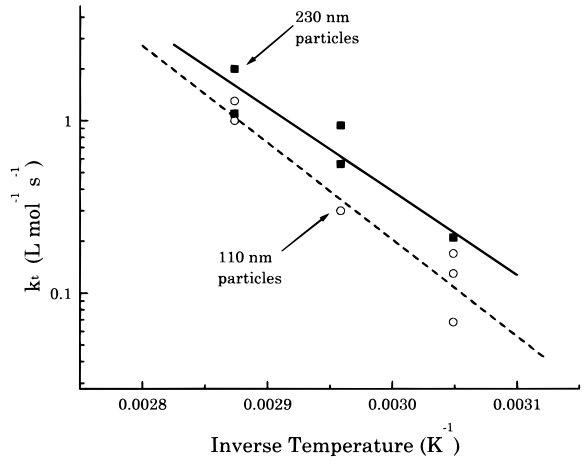

Figure 4. Arrhenius plot [ln(k_t) vs inverse temperature] for the long time k_t values, 110 (○) and 230 nm (■) PMMA particles.

Table 2. Activation Energies for Termination at Long Time

particle size, nm	E_a, kcal/mol	log(A_f)
110	25.9 ± 3.5	18.0 ± 2.2
230	22.6 ± 3.5	16.1 ± 2.3

constant rate coefficient. If we assume the rate law of eq 1, we can derive rate coefficient values at different times from the data. Figure 5 shows rate coefficient values at different times after the peak radical concentration for the 230 nm particle diameter long hold samples. The temperature was not held constant during this part of the run but ranged between ~50 and 58 °C. Therefore, these values are best compared with the 55 °C region 2 rate coefficient, which is shown at the far right in Figure 5. There is a fair amount of scatter in the time-dependent rate coefficient values, but qualitatively it is quite clear that in region 1 the rate coefficient falls by ~1−2 orders of magnitude during a period of ~10−20 min. The rate coefficient values at 20 min after the peak radical concentration time are ~3−5 times larger than the region 2 rate coefficient values.

Interpretation of Rate Coefficients: Estimation of w_p Values

As will become evident, precise, accurate w_p data are necessary for a good critical evaluation of the derived

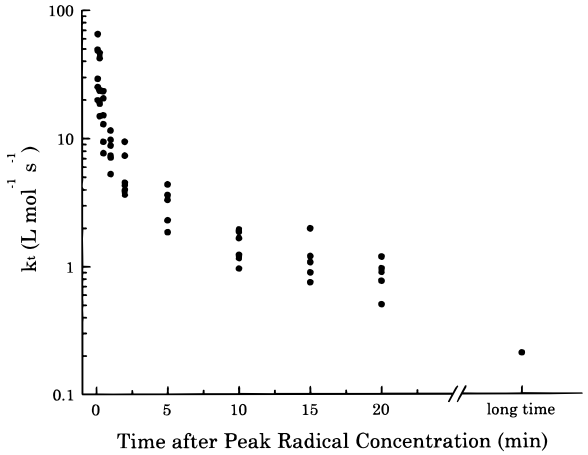

Figure 5. Values of k_t vs time after the peak radical concentration for 230 nm PMMA particles.

k_t values. As described in ref 6, w_p was monitored throughout the polymerizations by solids content and/or residual monomer analysis by GC. There are two problems with evaluating the k_t values using the experimentally determined w_p values alone. First, these w_p values have an uncertainty of ~±0.02—low on an absolute scale but large enough to hamper comparisons and interpretations in the high-conversion region. Second, the experimental w_p values are rather sparse.

We augmented the experimental w_p data as follows. First, using the measured w_p values as a guide, we assumed a w_p value (or range of w_p values) at a given time, t, on the [R•] vs time curve. From this w_p value, we derived [M$_t$], monomer concentration at time t. (We assumed that the monomer concentration is homogeneous in these simulations and in all of the analyses reported here.) We could then estimate the amount of monomer consumed as the polymerization progressed from time t by numerically integrating the equation

$$d[M]/dt = -k_p[M][R^\bullet] \quad (3)$$

with [M] = [M$_t$] at the start of the integration. To estimate k_p, we used a relationship between k_p and w_p that was derived by Russell et al.[8] from experimental data of Ballard et al.:[9]

$$k_p = k_p^0 \exp(-29.8(w_p - 0.84)) \quad (4)$$

with k_p^0 = 580 L mol^{-1} s^{-1} at 50 °C. Both the k_p data of Ballard et al.[9] and predictions from the $k_p - w_p$ relationship[8] agree well with k_p data for the systems studied here.[6]

As an example, we assume that $w_p = 0.95$ at the time when the flow was stopped and temperature set for one of the 55° long hold runs. We also assume a starting value for [R•] of 1×10^{-4} M (as suggested by the data). Then, 20 min after the temperature set time $w_p = 0.984$ and 50 min afterward $w_p = 0.994$. This relatively rapid monomer consumption is driven partly by the relatively high value of [R•]. Repeating the integration with the starting point [R•] = 1×10^{-5} M gives w_p values of 0.960 and 0.968 at 20 and 50 min, respectively.

Interpretation of Rate Coefficients: Comparisons with Other Values

Here we compare our k_t values from regions 1 and 2 with other experimental values and predictions from the

residual termination theory of Russell et al.[8] Comparisons between experimental values are somewhat problematical because of w_p and temperature differences. However, we can use the residual termination theory to predict how these differences will affect k_t.

The theory estimates residual termination rate coefficient, k_t^{res}, as follows. It is assumed that, at high conversion, the only way that the radical chain ends can approach each other is by adding monomer. Therefore, the termination rate is controlled by the propagation rate and monomer concentration. Russell et al.[8] give the following expression for k_t^{res} at high conversion:

$$k_t^{res} = 2\pi k_p[M]a^2\sigma/3 \quad (5)$$

Here k_p is the propagation coefficient, [M] is the monomer concentration, a is the polymer characteristic ratio, and σ is the monomer Lennard-Jones parameter. To estimate k_t^{res} for PMMA, we used the $k_p - w_p$ relationship and a and σ values given by Russell et al.[8]

The w_p dependence of k_t^{res} is obvious from eq 5 and the observed w_p dependence of k_p. Equation 5 implies a fairly simple temperature dependence for k_t^{res} as well. From eq 4, k_t^{res} and k_p must have the same temperature dependence. We know that at high conversion k_p is controlled by monomer diffusion. So k_p, and thus k_t^{res}, must have the same temperature dependence as monomer diffusion. (We shall see that, for PMMA, the activation energy for monomer diffusion at high conversion is much higher than the "chemical" propagation activation energy of ~5 kcal/mol measured at low conversion.[10])

We calculated an activation energy for MMA monomer diffusion in PMMA polymer of 26.7 kcal/mol from data measured in a recent study.[11] (Methanol diffusion in PMMA was measured in the same study; both the diffusion coefficients and their temperature dependence agreed well with literature data.) Note that this estimate of the MMA monomer diffusion activation energy is in very close agreement with the termination activation energy estimates of ~25 kcal/mol shown in Table 2. Also, both activation energy estimates are very similar to a recently reported value of 26 kcal/mol for the polymerization activation energy for diethylene glycol diacrylate (DEGDA).[12] The bulk polymerized reaction mixture gelled at fairly low (formal) conversion, presumably because the monomer is difunctional. So the reported activation energy is one appropriate for polymerization in a highly viscous medium, where monomer is not very mobile—a medium similar to our high-conversion PMMA.

There are a few estimates of k_t for PMMA in the literature. Ballard et al.[13] determined termination rate coefficients as a function of w_p in emulsion polymerized PMMA at 50 °C; their values extend to $w_p \cong 0.9$. Carswell et al.[14] used ESR measurements of [R•] as a function of time to determine termination and propagation rate coefficients for bulk polymerized PMMA at 60 °C. Their k_t value was measured at a somewhat lower conversion (they report $w_p = 0.90-0.95$) than the ones reported here. Cutting and Tabner[15] determined termination rate coefficients for emulsion polymerized PMMA at three different particle size/temperature combinations: 72 nm/60 °C, 135 nm/55 °C, and 240 nm/50 °C. The value of w_p for all polymerizations was in the range 0.95−0.98. Plonka et al.[16] determined termination rate coefficients for PMMA samples that were prepared by γ-radiation-induced bulk polymerization, annealed to remove postpolymerization radicals, and then irradiated with UV light. They followed the decay of the radicals produced by the UV irradiation at several different temperatures. Plonka et al.[16] did not give w_p values for their samples; however, on the basis of polymerization conditions and the reported sample T_g, knowledgeable sources[17] estimate that $w_p = 0.99-0.995$. Termination in these samples could not be described by a constant rate coefficient. It could be described by a time-dependent rate coefficient, similar to the rate coefficient behavior seen in the rapid termination period for our samples.

Table 3. High-Conversion PMMA Termination Rate Coefficients

source	k_t, L mol^{-1} s^{-1}	w_p	T, °C
Time-Independent			
this work, 110 nm particle	0.12	0.985−0.995	55
	0.30		65
	1.2		75
this work, 230 nm particle	0.21	0.985−0.995	55
	0.75		65
	1.6		75
Ballard et al.[13]	143	0.9	50
Carswell et al.[14]	3.5	0.90−0.95	60
Cutting and Tabner,[15] 72 nm particle	410	0.95−0.98	60
Cutting and Tabner,[15] 135 nm particle	35		55
Cutting and Tabner,[15] 240 nm particle	5		50
residual termination theory[8]	26	0.91	50
	11	0.93	
	4.5	0.95	
	1.5	0.97	
	0.28	0.99	
	0.12	0.995	
Time-Dependent			
this work, time = 0.1 min after peak radical concn	39.6 ± 17.5	0.906−0.932	~50−58
this work, time = 0.25 min	28.3 ± 13.0	0.912−0.934	
this work, time = 0.5 min	14.9 ± 6.2	0.920−0.938	
this work, time = 1 min	8.34 ± 2.21	0.931−0.944	
this work, time = 2 min	5.55 ± 2.34	0.942−0.951	
this work, time = 5 min	3.31 ± 1.05	0.958−0.964	
this work, time = 10 min	1.47 ± 0.41	0.969−0.974	
this work, time = 15 min	1.17 ± 0.43	0.976−0.980	
this work, time = 20 min	0.88 ± 0.23	0.980−0.983	
Plonka et al.,[16] time = 1 min	1.4	0.99−0.995	
Plonka et al.,[16] time = 2 min	1.1		
Plonka et al.,[16] time = 5 min	0.74		
Plonka et al.,[16] time = 10 min	0.56		
Plonka et al.,[16] time = 20 min	0.43		

Table 3 compares termination rate coefficients from the different sources. Time-independent rate coefficients are listed first, followed by the time-dependent ones. The w_p values for our samples were estimated using the numerical integration method described above and the following assumptions: (1) For the time-independent (region 2) rate coefficients, $w_p = 0.95$ at the temperature set time. Data from times less than 20 min after the temperature set time were excluded from the analysis. (2) For the time-dependent (region 1) rate coefficients, $w_p = 0.90-0.93$ at the time when the radical concentration peaked. (3) Because temperature = 55 °C, the k_p values determined from eq 4 must be multiplied by a factor of 1.8 (appropriate for an activation energy of 25 kcal/mol).

Figures 6 and 7 allow graphical comparison of the rate coefficients from the different sources. Figure 6 shows all of the Table 3 k_t data except the region 1 values from

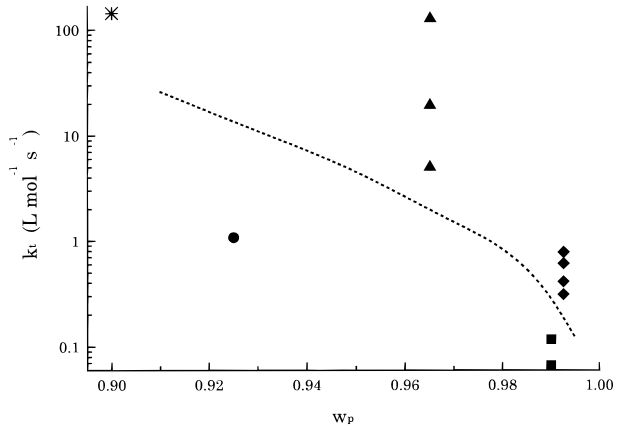

Figure 6. Comparison of region 2 k_t values (this work) with other experimental values and with predictions from the residual termination theory: - - -, theory; *, Ballard et al.;[13] ●, Carswell et al.;[14] ▲, Cutting and Tabner;[15] ◆, Plonka et al.;[16] ■, this work (region 2).

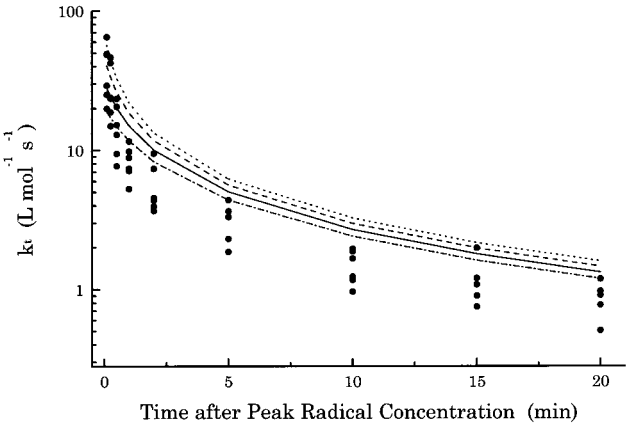

Figure 7. Comparison of region 1 k_t values (●) with predictions from the residual termination theory: - - -, $w_p = 0.90$; − − −, $w_p = 0.91$; —, $w_p = 0.92$; − - −, $w_p = 0.93$.

this work, as a function of w_p, all corrected to 50 °C assuming an activation energy of 25 kcal/mol. Figure 7 compares the region 1 k_t values as a function of time with predictions from the residual termination theory for $w_p = 0.90-0.93$ at 55 °C.

In Figure 6, the residual termination theory predictions split the experimental rate coefficients: values from this work and those of Carswell et al.[14] are lower than the predictions, while those of Ballard et al.,[13] Cutting and Tabner,[15] and Plonka et al.[16] are higher. The Cutting and Tabner[15] values may not be true residual termination coefficients: these polymerizations were run so that the initiator was still producing radicals at the time that k_t was measured. We suspect that these k_t values are dominated by short−long and perhaps short−short termination. The Plonka et al.[16] values may not be true residual termination coefficients either. It is difficult to reconcile the magnitude of these k_t values, their rapid decrease with time, and the very low levels of residual monomer in the context of the residual termination theory. The k_t values of Carswell et al.[14] and from region 2 of this work suggest that the residual termination theory overestimates the residual termination rate coefficient somewhat.

Figure 7 shows that in region 1 the k_t values fall off somewhat more rapidly than the residual termination theory suggests—consistent with the k_t values from region 2, as shown in Figure 6. This behavior is consistent with (but does not prove) a scenario in which (1) the residual termination rate coefficients in our systems are somewhat smaller than the theoretical prediction and (2) short−long termination (or some other termination mechanism) contributes to the total termination at short times.

Table 4. $\langle 1/i^2 \rangle$ Values Derived from Rapid Termination Rate Coefficients

time after peak [R•], min	$\langle 1/i^2 \rangle$ (peak $w_p = 0.90$)	$\langle 1/i^2 \rangle$ (peak $w_p = 0.93$)
0.1	0.27	0.58
0.25	0.23	0.45
0.5	0.15	0.26
1	0.12	0.18
2	0.11	0.15
5	0.11	0.13

Interpretation of Rate Coefficients: Comparison with Predictions from Chain-Length-Dependent Termination Theory

The comparisons above show that if we assume that the region 2 termination is residual, then the region 1 termination is probably too fast to be residual also. Qualitatively, the region 1 termination mode could be short−long: short−long termination is faster than residual termination. Short radicals could come from initiator, transfer events, or some other source. The observed increase in [R•] immediately before region 1 shows that there is some source of radicals in the system; some of these radicals almost certainly start life as "shorts".

To determine whether the region 1 termination rate coefficients are (semi)quantitatively consistent with short−long termination, we compared them with predictions made using an expression for the average short−long termination coefficient (k_t^{sL}) derived from chain-length-dependent termination theory:[4,5]

$$k_t^{sL} = k_p \langle 1/i^2 \rangle \qquad (6)$$

[The derivation of this expression is shown in the Appendix (Supporting Information).] Here, i is the length of a short chain; $\langle 1/i^2 \rangle$ is the average of the inverse of i^2. So $\langle 1/i^2 \rangle$ gives us a rough estimate of the average length of a "short". Physically, we know that $\langle 1/i^2 \rangle$ should be ≤ 1. Some rough comparisons with the chain-length-dependent termination theory suggest that $\langle 1/i^2 \rangle$ should also be $\geq \sim 0.01$ for very high conversions (otherwise k_t^{sL} becomes less than k_t^{res}, which is inconsistent with the theory).

Table 4 shows values of $\langle 1/i^2 \rangle$ derived from the rapid termination rate coefficients and w_p values shown in Table 3. To estimate k_p, we used the $k_p - w_p$ relationship of Russell et al.[8] and multiplied by 1.8 to account for the assumed temperature of 55 °C.

Derived $\langle 1/i^2 \rangle$ values are in the range $\sim 0.5-0.1$, which implies that the "shorts" are $\sim 1-3$ monomer units long. So it appears that the rapid termination rate coefficients are quantitatively consistent with short−long termination termination theory.

Discussion: Small vs Large Particles

The difference between the region 2 (slow) termination rate coefficients for the small and large particles is probably a consequence of the small difference in w_p values at very long reaction times. The smaller particles

tend to have slightly higher w_p values at long times and at "complete" conversion.

The dependence of region 1 (rapid) termination on particle size is qualitatively consistent with short−long termination occurring in this region. As ref 6 shows, region 1 is observed for particle diameters ≥170 nm, but not for particle diameters ≤120 nm. Short−long termination could be caused by inhomogeneous radical distribution in the larger particles.

The literature suggests that the distribution of radicals in latex particles can be inhomogeneous. Recent work by Mills et al.,[18,19] De la Cal et al.,[20] and Chern and Poehlein[21] suggests that the physical source of the distribution inhomogeneity is "surface anchoring": chains have an end group from the water-soluble initiators, and this end group wants to stay at the particle surface. Theoretically, surface anchoring could occur in our systems, which were made with a persulfate initiator. Surface anchoring implies that radical distribution will become more inhomogeneous as particle size increases.

Inhomogeneous radical distribution would be expected to enhance the rate of short−long termination, especially in systems where the "shorts" are quite short, as they appear to be in our systems. A "short" can either add monomer or terminate a "long". For short−long termination to occur at all, the "short" has to encounter a "long" before it has added enough monomers to become a "long" itself. This implies that short−long termination does not occur below a certain threshold radical concentration.

This concept of a threshold radical concentration for short−long termination can explain why short−long termination could occur in our systems when it has not previously been observed in PMMA. [R•] values in our systems are on the high side, $\sim 10^{-4}$ mol/L. This is about an order of magnitude higher than the [R•] values reported for the systems of Cutting and Tabner[15] and Carswell et al.[14]

Our hypothesis is that radical distribution inhomogeneities increase the radical concentration above the short−long threshold in parts of the large particles, but not in the smaller ones. A piece of evidence in support of this hypothesis is that we can induce a region 1 in the small particle [R•] vs time data by doubling the initiator concentration.[22]

Inhomogeneous radical distribution could also increase the apparent rate of residual termination. We ran some model calculations to see whether distribution-inhomogeneity-enhanced residual termination is a reasonable explanation for the observed region 1 termination. Our model assumed a core−shell model for the individual particles with the radical concentration being higher in the outer shell than in the core. We also assumed that residual termination is the only mechanism in both shell and core. We then estimated the shell thickness which would be necessary to give the termination rates observed in region 1.

The estimation procedure is described in the Appendix. The shell thickness depends on F, the fraction of [R•] which is in the shell; k_t/k_t^{res}, the ratio of the observed to the true residual termination coefficient; and the particle radius. $F = 0.1-0.3$ is a reasonable range; typically, [R•] decreases by 10−30% during region 1. Given the differences between the region 1 and 2 termination rate coefficients, we felt that $k_t/k_t^{res} = 1.5-10$ is a reasonable range. Table 5 shows Fr_{shell}, the ratio of the shell thickness to the particle radius, for these ranges.

Table 5. Fr_{shell} Values Derived Assuming Radical Distribution Inhomogeneity and Residual Termination

k_t/k_t^{res}	$F = 0.10$	$F = 0.20$	$F = 0.30$
10	3.63×10^{-4}	1.43×10^{-3}	3.17×10^{-3}
8	4.64×10^{-4}	1.82×10^{-3}	4.01×10^{-3}
6	6.43×10^{-4}	2.50×10^{-3}	5.48×10^{-3}
4	1.05×10^{-3}	3.99×10^{-3}	8.65×10^{-3}
2	2.83×10^{-3}	1.00×10^{-2}	2.07×10^{-2}
1.5	4.94×10^{-3}	1.64×10^{-2}	3.23×10^{-2}

Based on Table 5, the assumption of residual termination only in a core−shell morphology implies a very thin shell. For a 200 nm particle, the Table 5 Fr_{shell} values imply shell thicknesses in the 0.04−3.2 nm range. These thicknesses seem small—they are less than the calculated R_g for PMMA with MW ≅ 10^6. So while we cannot rule out radical-distribution-inhomogeneity-enhanced residual termination as the sole explanation for region 1, it does not look too reasonable quantitatively.

Conclusions

For both 110 and 230 nm particle size emulsion polymerizations of MMA, at long times (very high conversion) we observed a slow termination (region 2) for which the functional form is consistent with that for bimolecular termination with a constant rate coefficient. We derived termination rate coefficients which are at least qualitatively consistent with previously reported values for the high-conversion termination rate coefficient in PMMA[13−16] and predictions of the residual termination theory.[8] Comparison of the k_t values determined here with those determined by others and with the predictions of the residual termination theory points out the strong influence that w_p has on very high conversion k_t values. The activation energy for the slow termination is very similar to the activation energy for MMA diffusion in PMMA. This similarity is also consistent with the residual termination theory. We conclude that the slow termination is residual termination.

For 230 nm particles, at shorter times (still high conversion) we observed a rapid termination (region 1) whose functional form is not consistent with that for bimolecular termination with a constant rate coefficient. A time-dependent k_t model fits our data well. Because there was some minor temperature variation during the rapid termination period, and because we do not know w_p at the radical peak with high precision, we cannot absolutely rule out residual termination as the sole termination mechanism throughout the rapid termination period. However, there are inconsistencies between the rapid termination period data and the predictions of the residual termination theory. Our data are consistent with (but do not prove) short−long termination early in the rapid termination period.

A reasonable explanation for why we observe the rapid termination period in the 230 nm particles but not in the 110 nm particles is radical distribution inhomogeneities. If these are driven by surface anchoring effects, as recent work suggests,[18−21] then they will become more pronounced as particle size increases. The radical concentration will be increased in the outer shell of the particle. This type of radical concentration inhomogeneity would be expected to increase the apparent rates of both short−long and residual termination, but it may be that the inhomogeneity is allowing short−

long termination to be kinetically significant where otherwise it would not be. Consider that the data suggest that in PMMA the "shorts" are very short. Addition of just a few monomer units can turn a "short" into a "long". For short−long termination to be observed, significant numbers of "shorts" must encounter "longs" before the "shorts" add enough monomer to become "longs" themselves. This suggests that the radical concentration must be above a threshold level for short−long termination to be observed. Radical distribution inhomogeneities could push the concentration in the radical-enriched shell of the 230 nm particles, but not the 110 nm particles, above this level.

Acknowledgment. We acknowledge vital contributions to design of our original flow system by Willie Lau. We also acknowledge Prof. Bob Gilbert for numerous stimulating technical discussions. Finally, we thank the Rohm and Haas Co. for support of this work and permission to publish.

Supporting Information Available: Derivations of the average short−long termination coefficient and the shell thickness for radical inhomogeneity-enhanced residual termination. This material is available free of charge via the Internet at http://pubs.acs.org.

References and Notes

(1) Gilbert, R. G. *Emulsion Polymerization: A Mechanistic Approach*; Academic: London, 1995.
(2) O'Shaughnessy, B.; Yu, J. *Macromolecules* **1994**, *27*, 5067.
(3) O'Shaughnessy, B.; Yu, J. *Macromolecules* **1994**, *27*, 5079.
(4) Russell, G. T.; Gilbert, R. G.; Napper, D. H. *Macromolecules* **1992**, *25*, 2459.
(5) Russell, G. T.; Gilbert, R. G.; Napper, D. H. *Macromolecules* **1993**, *26*, 3538.
(6) Parker, H.-Y.; Westmoreland, D. G.; Chang, H.-R. *Macromolecules* **1996**, *29*, 5119.
(7) *SAS User's Guide: Statistics. Version 5 Edition*, SAS Institute, Inc., Box 8000, Cary, NC 27511-8000.
(8) Russell, G. T.; Napper, D. H.; Gilbert, R. G. *Macromolecules* **1988**, *21*, 2133.
(9) Ballard, M. J.; Napper, D. H.; Gilbert, R. G. *J. Polym. Sci., Polym. Chem. Ed.* **1984**, *22*, 3225.
(10) Hutchinson, R. A.; Aronson, M. T.; Richards, J. R. *Macromolecules* **1993**, *26*, 6410.
(11) Xie, L. Q. *Polymer* **1993**, *34*, 4579.
(12) Thakur, A.; Banthia, A. K.; Maiti, B. R. *J. Appl. Polym. Sci.* **1995**, *58*, 959.
(13) Ballard, M. J.; Napper, D. H.; Gilbert, R. G. *J. Polym. Sci., Part A: Polym. Chem.* **1984**, *22*, 3225.
(14) Carswell, T. G.; Hill, D. J. T.; Londero, D. I.; O'Donnell, J. H.; Pomery, P. J.; Winzor, C. L. *Polymer* **1992**, *33*, 137.
(15) Cutting, G. R.; Tabner, B. J. *Macromolecules* **1993**, *26*, 951.
(16) Plonka, A.; Bednarek, J.; Pietrucha, K. *J. Chem. Phys.* **1996**, *104*, 5279.
(17) Cholod, M. B.; Shah, N., private communication.
(18) Mills, M. F.; Gilbert, R. G.; Napper, D. H. *Macromolecules* **1990**, *23*, 4247.
(19) Mills, M. F.; Gilbert, R. G.; Napper, D. H.; Rennie, A. R.; Ottewill, R. H. *Macromolecules* **1993**, *26*, 3553.
(20) De la Cal, J. C.; Urzay, R.; Zamora, A.; Forcada, J.; Asua, J. M. *J. Polym. Sci., Part A: Polym. Chem.* **1990**, *28*, 1011.
(21) Chern, C. S.; Poehlein, G. W. *J. Polym. Sci., Part A: Polym. Chem.* **1987**, *25*, 617.
(22) Chang, H.-R.; Parker, H.-Y.; Westmoreland, D. G., unpublished results.
(23) Russell, G. T.; Napper, D. H.; Gilbert, R. G. *Macromolecules* **1988**, *21*, 2133.

MA980230M